ORIGINAL ARTICLE

Molecular Plant Pathology   WILEY

LsGRP1, a class II glycine-rich protein of *Lilium*, confers plant resistance via mediating innate immune activation and inducing fungal programmed cell death

Chia-Hua Lin [ID] | Ying-Chieh Pan | Nai-Hua Ye | Yu-Ting Shih | Fan-Wei Liu | Chao-Ying Chen [ID]

Department of Plant Pathology and Microbiology, National Taiwan University, Taipei, Taiwan

Correspondence
Chao-Ying Chen, Department of Plant Pathology and Microbiology, National Taiwan University, No. 1, Sec. 4, Roosevelt Rd., Taipei 10617, Taiwan.
Email: cychen@ntu.edu.tw

Funding information
Ministry of Science and Technology, Taiwan

Abstract

Defence-related LsGRP1 is a leaf-specific plant class II glycine-rich protein (GRP) involved in salicylic acid-induced systemic resistance against grey mould caused by necrotrophic *Botrytis elliptica* in lily (*Lilium*) cultivar Stargazer. The C-terminal region of LsGRP1 (LsGRP1^C) can inhibit fungal growth in vitro via a mechanism of inducing fungal apoptosis programmed cell death (PCD). In this study, the role of LsGRP1 in induced defence mechanism was investigated using *LsGRP1*-silenced Stargazer lily and *LsGRP1*-transgenic *Arabidopsis thaliana*. *LsGRP1* silencing in lily was found to slightly inhibit plant growth and greatly increase the susceptibility to *B. elliptica* by suppressing callose deposition and early reactive oxygen species (ROS) accumulation. In contrast, *LsGRP1*-transgenic *Arabidopsis* showed higher resistance to *Botrytis cinerea* and also to *Pseudomonas syringae* pv. *tomato* DC3000 as compared to the wild type, accompanied with the enhancement of callose deposition and ROS accumulation. Additionally, *LsGRP1* silencing increased plant cell death caused by *B. elliptica* secretion and reduced pathogen-associated molecular pattern (PAMP)-triggered defence activation in Stargazer lily. Consistently, *LsGRP1* expression boosted PAMP-triggered defence responses and effector recognition-induced hypersensitive response in *Arabidopsis*. Moreover, fungal apoptosis PCD triggered by LsGRP1 in an LsGRP1^C-dependent manner was demonstrated by leaf infiltration with LsGRP1^C-containing recombinant proteins in Stargazer lily. Based on these results, we presume that LsGRP1 plays roles in plant defence via functioning as a pathogen-inducible switch for plant innate immune activation and acting as a fungal apoptosis PCD inducer to combat pathogen attack.

KEYWORDS
host-induced fungal apoptosis programmed cell death, innate immune activation, LsGRP1, plant class II glycine-rich protein

---

1 | INTRODUCTION

Plants have evolved a complex innate immune system comprising two major branches to protect themselves against diverse pathogenic invaders. The first branch is pattern-triggered immunity (PTI), which is evoked on the perception of pathogen-, microbe-, or damage-associated molecular patterns (PAMPs/MAMPs/DAMPs) by the plasma membrane-associated pattern-recognition receptors (PRRs), and activates defence responses such as reactive oxygen species (ROS) accumulation, callose deposition, antimicrobial compound production, defence hormone signalling, and transcriptional reprogramming (Bigeard *et al*., 2015; Peng *et al*., 2018; Zhang *et al*., 2018; Noman *et al*., 2019). However, host-adapted pathogens have developed various effectors capable of countering PTI. In turn, plants detect effectors with their corresponding evolved cytoplasmic receptors, classically known as resistance proteins (R proteins), to activate the second innate immune branch named effector-triggered immunity (ETI). ETI is regarded as an accelerated and amplified PTI response with shared signalling mechanisms and often leads to a hypersensitive response (HR) and systemic acquired resistance, a form of induced resistance to prevent secondary infections (Peng *et al*., 2018; Zhang *et al*., 2018; Noman *et al*., 2019). HR is a unique plant programmed cell death (PCD), occurring at or around pathogen penetration sites, capable of preventing infection but beneficial for certain necrotrophic pathogens (Balint-Kurti, 2019; Lorang, 2019). Pathogen recognition alters the expression of approximately 20% of total genes in a single plant species, and a proper plant transcriptional reprogramming is critical for orchestrating effective defence responses and minimizing fitness cost (Bigeard *et al*., 2015; Zhang *et al*., 2018).

Induced resistance, a physiological state of enhanced defensive capacity developed on certain stimulators, is a fitness optimization strategy of a plant to achieve growth and defence balance in response to resource restrictions (Heil and Baldwin, 2002; Walters and Heil, 2007). Defence priming is an intrinsic part of induced resistance, which remarkably triggers direct changes crucial for the enhanced defensive behaviour rather than directly launching induced defences (Mauch-Mani *et al*., 2017). Accordingly, the genes involved in defence priming presumably play a decisive role in the enhanced activation of induced defence mechanisms and are desirable options for the research of growth–defence trade-offs and the resource of disease resistance breeding. Plant immunity to date is mainly investigated in dicot species, especially the model plant *Arabidopsis*, as well as cereal monocot species (family Poaceae), but rarely expounded in noncereal monocot species. However, the hormone-mediated defence networking in rice is found distinct from that found in *Arabidopsis* (de Vleesschauwer *et al*., 2013, 2014). Taken together, it is suggested that some defence genes employed in the induced resistance of monocot species, especially noncereal ones, probably play uncharacterized roles in defence activation.

Lily, the common name for the perennial herbaceous monocotyledonous genus *Lilium*, is an important floral crop consisting of approximately 100 known species and thousands of cultivars, which are classified into nine horticultural divisions based on the wild parent species (van Tuyl and Arens, 2011). The *Lilium*-specific necrotrophic fungus *Botrytis elliptica* causes the most destructive and dominant disease of lily worldwide called grey mould, also known as leaf blight or fire blight (Staats *et al*., 2005). The host specialization and pathogenicity of *B. elliptica* could be determined by some secreted fungal proteins essential for the induction of lily apoptosis PCD, which enables the subsequent infection (van Baarlen *et al*., 2004). Most commercially available lily cultivars are highly vulnerable to *B. elliptica*, except several Oriental hybrid cultivars (division 7) that show reduced necrotic symptoms probably related to the rapid accumulation of ROS (Balode and Belicka, 2004; Daughtrey and Bridgen, 2013; Gao *et al*., 2018), implying a genetic background of grey mould resistance in this division. Additionally, the Oriental hybrid cultivar Stargazer with lower *B. elliptica* susceptibility can be even enhanced in grey mould resistance by the pretreatments of salicylic acid (SA) and the plant defence activator probenazole, accompanied by the increased expression of *LsGRP1* (accession number AY072283) (Chen *et al*., 2003; Lu and Chen, 1998, 2005; Lu *et al*., 2007). *LsGRP1* gene expression and protein accumulation in *Lilium* cultivar Stargazer are maintained at basal levels under normal growth conditions and up-regulated by SA treatment and *B. elliptica* challenge. Leaf-specific LsGRP1 is a 138-amino acid plant class II glycine-rich protein (GRP) with the typical composition of an N-terminal signal sequence, a central glycine-rich domain, and a C-terminal cysteine-rich region (LsGRP1^C), and is distributed in plasma membrane and cell walls (Lu and Chen, 2005; Lu *et al*., 2007; Lin and Chen,2014, 2017). Synthetic LsGRP1^C and *Escherichia coli*-expressed LsGRP1^C recombinant protein exhibit antimicrobial activity against bacterial and fungal microorganisms in vitro via the mechanism of causing microbial membrane permeabilization and inducing fungal apoptosis PCD (Lin *et al*., 2014, 2017). Recently, phytoalexin camalexin-induced fungal apoptosis PCD has been regarded as a defence mechanism of *Arabidopsis* to combat necrotrophic *Botrytis cinerea* (Shlezinger *et al*., 2011a, 2011b; Veloso and van Kan, 2018), a polyphagous species of the genus *Botrytis* capable of causing grey mould in over 200 eudicot species (Staats *et al*., 2005). According to the expression profile and biochemical characteristics, LsGRP1 is strongly suggested to be involved in the induced defence mechanism of lily.

Several plant class II GPRs are reported to be involved in various biotic and abiotic stress responses. *Arabidopsis AtGRP3* is an SA-induced gene specifically expressed in leaves and stems (de Oliveira *et al*., 1990). Extracellular AtGRP3 and its interactor KAPP, a cytoplasmic plasma membrane-localized kinase-associated protein phosphatase, negatively affect the basal resistance to *B. cinerea* and the induction of callose deposition, ROS accumulation, and defence gene expression by wounding, DAMP oligogalacturonides, and the bacterial PAMP flg22. However, the other AtGRP3 interactor AtWAK1, a cell wall-associated receptor-like kinase serving as an oligogalacturonide receptor, acts conversely except that it is unresponsive to flg22 (Park *et al*., 2001; Yang *et al*., 2003; Gramegna *et al*., 2016). In addition, AtGRP3/AtWAK1 interaction is involved in root size determination and aluminium response (Park *et al*., 2001;

Mangeon *et al.*, 2016, 2017). However, AtGRP3 enables defence induction of callose deposition and ROS accumulation through directly interacting with the bacterial elicitor HrpE, which presents in type III protein secretion pilus of *Xanthomonas citri* subsp. *citri* and can also interact with CsGRP, a class II GRP of citrus (Gottig *et al.*, 2018). Similarly, *Nicotiana tabacum* cdiGRP is up-regulated under cadmium stress, and its accumulation in cell walls blocks the systemic infection of tobamovirus via enhancing vascular callose deposition (Ueki and Citovsky,2002, 2005). In terms of abiotic stress, apoplast-accumulated CpGRP1 of *Craterostigma plantagineum* seems to play a central role in activating dehydration-related responses to water deficit through interacting with CpWAK1, an ortholog of *Arabidopsis* AtWAK2 (Giarola *et al.*, 2016; Jung *et al.*, 2019). Accordingly, the cell surface-localized plant class II GRPs, including LsGRP1 of lily, possibly mediate defence against diverse stresses while the corresponding defence activators appear.

In this study, to uncover the role of LsGRP1 in plant immunity, the effect of *LsGRP1* expression on disease resistance, defence activation, and fungal apoptosis PCD were investigated using *LsGRP1*-silenced lily and *LsGRP1*-transgenic *Arabidopsis* as well as lily leaf infiltration with LsGPP1-derived recombinant proteins. In addition, the involvement of LsGRP1 in innate immune activation was examined by assessing PTI- and ETI-associated defence responses elicited by the treatment of *B. elliptica* secretion PAMPs or effectors. Based on the results, the induced resistance-related LsGRP1 was presumed to act as a pathogen-inducible switch for innate immune activation and a fungal apoptosis PCD inducer in both monocot and dicot species, which is crucial for grey mould resistance in lily.

2 | RESULTS

2.1 | *LsGRP1* silencing slightly reduces lily growth and greatly increases lily susceptibility to *B. elliptica*

To investigate the involvement of LsGRP1 in lily immunity, grey mould resistance levels of *LsGRP1*-silenced and *LsGRP1*-nonsilenced lily plants were compared. *LsGRP1* expression of lily was silenced by *Agrobacterium*-mediated infection of tobacco rattle virus (TRV)-based virus-induced gene silencing (VIGS) vector system, which was shown to systemically silence the endogenous phytoene desaturase gene (*PDS*) of *Lilium* cultivar Stargazer in a preliminary assay (Figure S1). Interestingly, *LsGRP1*-silenced lily (VIGS-*LsGRP1*) showed a notable reduction in shoot length as compared to VIGS-control lily (VIGS-CK) as well as VIGS-untreated lily (Un-VIGS) (Figure 1a). The ratios of *LsGRP1* expression and LsGRP1 accumulation (the total amounts of 14-, 16-, and 23-kDa LsGRP1) in the leaves of VIGS-untreated lily, *LsGRP1*-silenced lily, and VIGS-control lily were determined to be 23.1:29.3:100 and 47.3:54.6:100, respectively, as detected by quantitative reverse transcription polymerase chain reaction (RT-qPCR) and western blot analysis (Figure 1b,c). In addition, the TRV amounts in *LsGRP1*-silenced lily and VIGS-control lily were equal but three-times higher than that in VIGS-untreated lily

(Figure 1b). It was noticed that an increased TRV titre led to a normal shoot length and a higher *LsGRP1* expression level (VIGS-CK vs. Un-VIGS) but brought about a reduced shoot length while *LsGRP1* was silenced to a similar expression level (VIGS-*LsGRP1* vs. Un-VIGS). Accordingly, it is presumed that *LsGRP1* expression promotes the shoot elongation of lily, and the normal shoot length of VIGS-control lily comes from the neutralization between viral infection-triggered inhibitory effect and the LsGRP1-triggered promoting effect.

B. elliptica in *LsGRP1*-silenced leaves had a biomass 2.8-fold higher than that in VIGS-control leaves at 1 day post-inoculation (dpi) (Figure 1d), and caused more water-soaked, expanding lesions at 3 dpi (Figure 1e, left panel). Trypan blue staining at 7 dpi revealed that lots of severe necrotic lesions (19.6%) appeared in *LsGRP1*-silenced leaves, whereas far fewer necrotic lesions (1.9%) and some HR occurred in VIGS-control leaves (Figure 1e, middle and right panels). Microscopical observation of trypan blue-stained leaves at 2 dpi clearly showed that *B. elliptica* proliferated well and caused plant necrotic cell death in *LsGRP1*-silenced leaves but was restricted and killed within an HR in VIGS-control leaves. In these HR sites, only very rare fungus-attacking lily cells were stained by trypan blue and most of them were enclosed by lily cells with an irreversibly browned appearance (Figure 1f). In addition, *LsGRP1*-silencing also accelerated the in planta sporulation of *B. elliptica* (Figure 1g). These findings reveal that LsGRP1 contributes to lily resistance against grey mould disease and is probably involved in lily growth.

2.2 | LsGRP1 mediates PTI-associated callose deposition and ROS accumulation crucial for counteracting *B. elliptica* infection in lily

To verify that LsGRP1 accumulation also triggers PTI-associated defence responses, callose deposition and ROS accumulation in leaves of *LsGRP1*-silenced and VIGS-control lily plants were compared after *B. elliptica* inoculation. Callose deposition and ROS accumulation were detected by aniline blue and 3,3′-diaminobenzidine (DAB) staining, respectively. In planta fungal proliferation and plant cell death were selectively detected by additional trypan blue staining. The effect of these plant defence responses on preventing *B. elliptica* infection and the requirement of LsGRP1 for awaking these defences were then assessed by the inhibitor assays.

In VIGS-control leaves, callose deposited in front of the hyphae of germinating spores to arrest fungal growth at 16 hr post-inoculation (hpi) became abundant and attempted to pack fungal hyphae in bales at 24 hpi, disappeared at 48 hpi, and appeared to surround the hyphae again at 72 hpi. By contrast, callose deposition was seldom found throughout these time points in *LsGRP1*-silenced leaves where spores germinated earlier and the fungus proliferated better (Figure 2a). Preinfiltration with 2-deoxy-D-glucose (2-DDG), a callose synthesis inhibitor, strongly suppressed callose deposition and enhanced fungal growth in lily leaves during the observation period within 68 hpi. Conversely, lots of callose was deposited in control leaves preinfiltrated with sterile deionized water at 12 hpi, which

seemed to prevent most spore attachments, and thus resulted in almost no spores being found on the leaf surface after the histochemical staining procedures. At 40 and 68 hpi, some callose still remained in control leaves to hinder *B. elliptica* infection (Figure 2b). In addition, *B. elliptica* in 2-DDG-treated leaves had a biomass 48% higher than that in control leaves at 68 hpi (Figure 2c) and caused a larger lesion at 7 dpi, on which *B. elliptica* had formed aerial mycelia, whereas the fungal growth was restricted inside the leaf tissues of control ones (Figure 2d). To further confirm the defensive function of LsGRP1 in

mediating callose deposition against *B. elliptica*, the callose deposition and necrotic lesions were compared in *LsGRP1*-silenced and VIGS-control leaves that were preinfiltrated with 2-DDG or sterile deionized water. *LsGRP1*-silencing and 2-DDG treatment caused 44.5% and over 70% decreases of callose deposition, respectively, at 16 hpi. The relative necrotic areas at 3 dpi showed negative correlations with the callose deposition levels (Figure 2e). LsGRP1 involvement in callose deposition essential for the restriction of *B. elliptica* was therefore demonstrated.
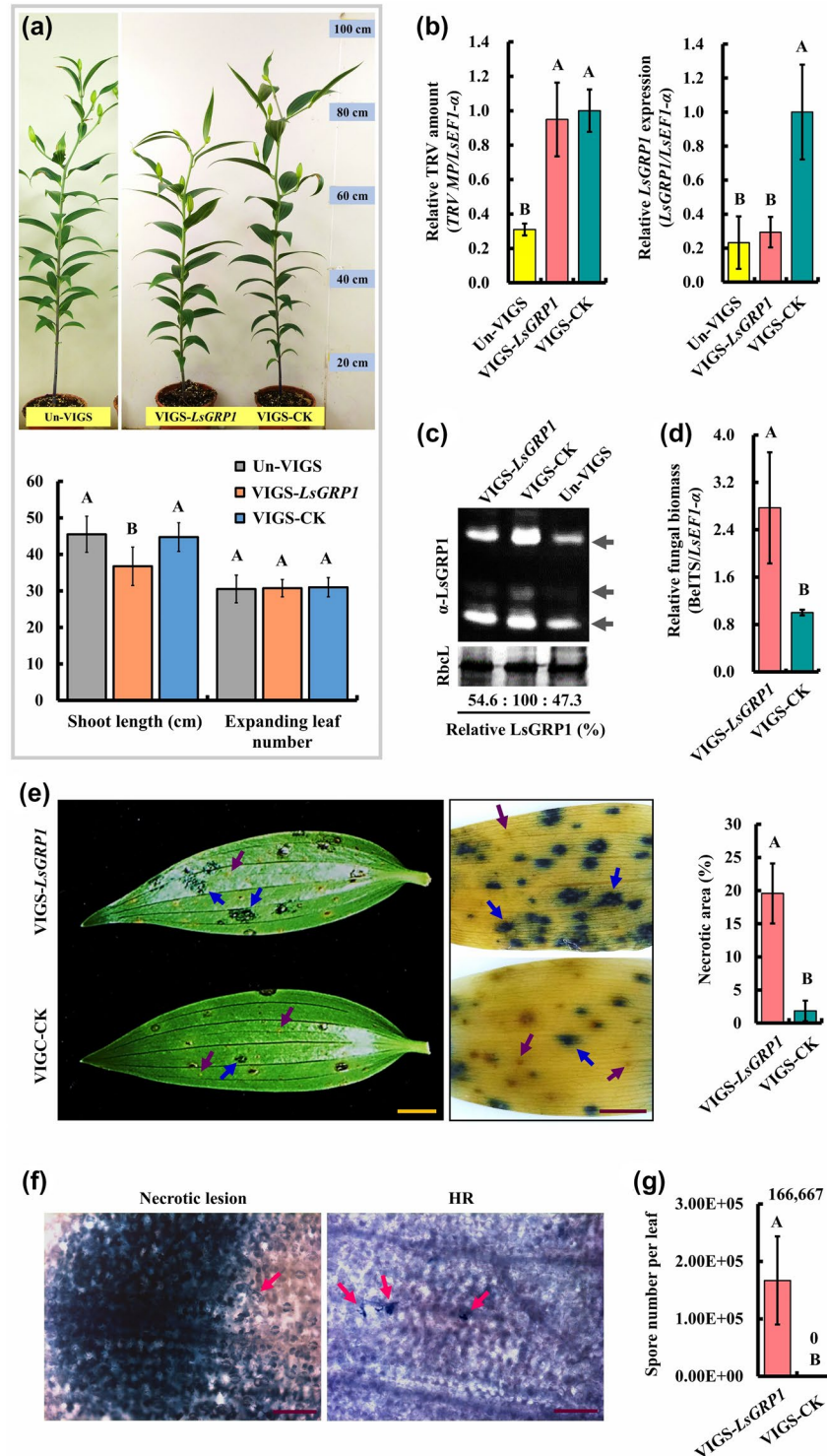
FIGURE 1 *LsGRP1* silencing increases lily susceptibility to grey mould caused by *Botrytis elliptica*. (a) The morphology of virus vector-untreated lily (Un-VIGS) and virus vector-treated *LsGRP1*-silenced (VIGS-*LsGRP1*) and VIGS-control (VIGS-CK) lilies at 8 weeks old (upper panel). *Agrobacterium*-mediated tobacco rattle virus (TRV) vector-induced gene silencing was performed 5 weeks before observation. The shoot length and expanding leaf number of 7-week-old lily plants are shown in lower panel. The levels of TRV vector, *LsGRP1* expression (b) and LsGRP1 accumulation (c) in leaves were detected by quantitative reverse transcription PCR and western blot analysis, respectively. (c) LsGRP1 of 24-, 16-, and 14-Da detected by LsGRP1[N] antibody (α-LsGRP1) indicated by arrows from top to bottom, and RuBisCO large subunit (RbcL) stained by Coomassie brilliant blue was used as a loading control. The *LsGRP1*-silenced and VIGS-control leaves were detached and droplet- (20 μl in [d] and [g]) or spray-inoculated ([e] and [f]) with spore suspension of *B. elliptica* at 5×10^4 spores/ml. (d) Relative *B. elliptica* biomass was detected by quantitative PCR at 1 day post-inoculation (dpi). (e) Symptom at 3 dpi (left panel) and trypan blue-stained host cell death at 7 dpi (middle panel). Necrotic lesions and hypersensitive responses (HR) are indicated by blue and purple arrows, respectively. The proportion of necrotic area at 7 dpi labelled by trypan blue was quantified (right panel). (f) Necrotic lesion in *LsGRP1*-silenced leaves and HR in VIGS-control leaves were microscopically observed at 2 dpi after trypan blue staining. *B. elliptica* is indicated by arrows. Bar: 2 cm in (e); 200 μm in (f). (g) In planta fungal sporulation occurred in *LsGRP1*-silenced leaves but not VIGS-control leaves at 10 dpi. Data represent the mean ± *SD* from four, four, three, five, and four biological replicates in (a), (b), (d), (e), and (g), respectively. Statistical analysis was performed using one-way analysis of variance (ANOVA) followed by Fisher's least significant difference (LSD) test ($p < .05$)

In terms of ROS accumulation, microscopical observation showed that ROS was detectable in VIGS-control leaves but not in *LsGRP1*-silenced leaves at 10 hpi. Although ROS increased in both VIGS-control and *LsGRP1*-silenced leaves at 16 hpi, it formed fewer spots with much more intense signals in VIGS-control lily leaves (Figure 3a), suggesting that a more accurate and strong ROS defence against *B. elliptica* challenge could be conducted by *LsGRP1* expression. The macro-view revealed that ROS accumulation in VIGS-control leaves had a higher level at 24 hpi and decreased at 48 hpi. However, ROS accumulation in *LsGRP1*-silenced leaves was delayed, and at 48 hpi it increased to a level close to that of VIGS-control leaves at 24 hpi (Figure 3b). Application of diphenyleneiodonium (DPI), a ROS generation inhibitor, abolished the ROS accumulation within 24 hpi and resulted in a better fungal proliferation and larger lesions as compared to control leaves preinfiltrated with 1% dimethyl sulphoxide (DMSO), the vehicle control (Figure 3c,d). To confirm the role of LsGRP1 in triggering early ROS generation against *B. elliptica*, the ROS accumulation and necrotic lesions were compared in *LsGRP1*-silenced and VIGS-control leaves that were preinfiltrated with DPI or 1% DMSO(Figure 3e). *LsGRP1*-silencing and DPI treatments both led to over 40% reductions of ROS accumulation at 16 hpi, and interestingly they caused 51.1% and over 85% increments in necrotic symptoms at 3 dpi, respectively, revealing that the *B. elliptica*-triggered defensive ROS generation in lily dependsgreatly on LsGRP1 accumulation. Accordingly, the contribution of LsGRP1 in mediating rapid and intense ROS accumulation at the sites of fungal attack to block *B. elliptica* was verified.

2.3 | LsGRP1 triggers *B. elliptica* to undergo apoptosis PCD in lily via the antimicrobial cysteine-rich C-terminal region

The cysteine-rich C-terminal region of LsGRP1, LsGRP1[C], was proven to inhibit fungal growth in vitro by triggering fungal apoptosis PCD (Lin et al.,2014, 2017). Because fungal apoptosis PCD induced by camalexin is regarded as a defence mechanism of *Arabidopsis*

against necrotrophic *B. cinerea* (Shlezinger *et al.*, 2011a,2011b; Veloso and van Kan, 2018), the involvement of LsGRP1 in lily-induced *B. elliptica* apoptosis PCD was investigated using a terminal deoxynucleotidyl transferase dUTP nick end-labelling (TUNEL) assay to detect chromosomal DNA fragmentation, a typical apoptosis PCD phenomenon.

First, to confirm the functional region of LsGRP1 critical for the induction of fungal apoptosis PCD, the apoptosis PCD level of *B. elliptica* hyphae was surveyed 1 day after the in vitro treatment with 10 μM of different LsGRP1-derived recombinant proteins. Not surprisingly, LsGRP1[C]-containing recombinant proteins of SUMO-LsGRP1 and SUMO-LsGRP1[C] were found to exhibit remarkable fungal apoptosis PCD-inducing activities, which caused 58.24% and 66.2% of fungal cells to undergo apoptosis PCD, respectively. By contrast, the removal of LsGRP1[C] (SUMO-LsGRP1ΔC) totally abolished this activity; the fungal apoptosis PCD incidence rate of SUMO-LsGRP1ΔC treatment was statistically identical to those of negative controls, including sterile deionized water and the N-terminal fusion partner SUMO of recombinant proteins (SUMO-CK) (Figure 4). Thus, LsGRP1[C] isfunctionally essential for LsGRP1 to induce fungal apoptosis PCD.

Because LsGRP1 has a cell surface localization (Lin and Chen, 2014), the fungal apoptosis PCD-inducing activity of LsGRP1[C] and its contribution to grey mould resistance of lily was further assessed by increasing LsGRP1[C] abundance by leaf infiltration with recombinant proteins at 1 hr before *B. elliptica* inoculation. Infiltration with SUMO-LsGRP1 and SUMO-LsGRP1[C] was found to greatly suppress fungal growth and induced fungal apoptosis PCD in lily leaves as compared to infiltration with sterile deionized water, SUMO-LsGRP1ΔC, or SUMO-CK (Figure 5). The fungal biomass detected by quantitative PCR and the fungal morphology visualized by trypan blue staining at 24 hpi revealed that LsGRP1-derived recombinant proteins inhibited the spore germination and the subsequent growth of *B. elliptica* in an LsGRP1[C]-dependent manner, whereas SUMO-CK treatment conversely promoted *B. elliptica* proliferation as compared to water treatment. Additionally, the TUNEL assay within 96 hpi indicated that the treatments of LsGRP1[C]-containing recombinant proteins specifically conferred higher fungal apoptosis
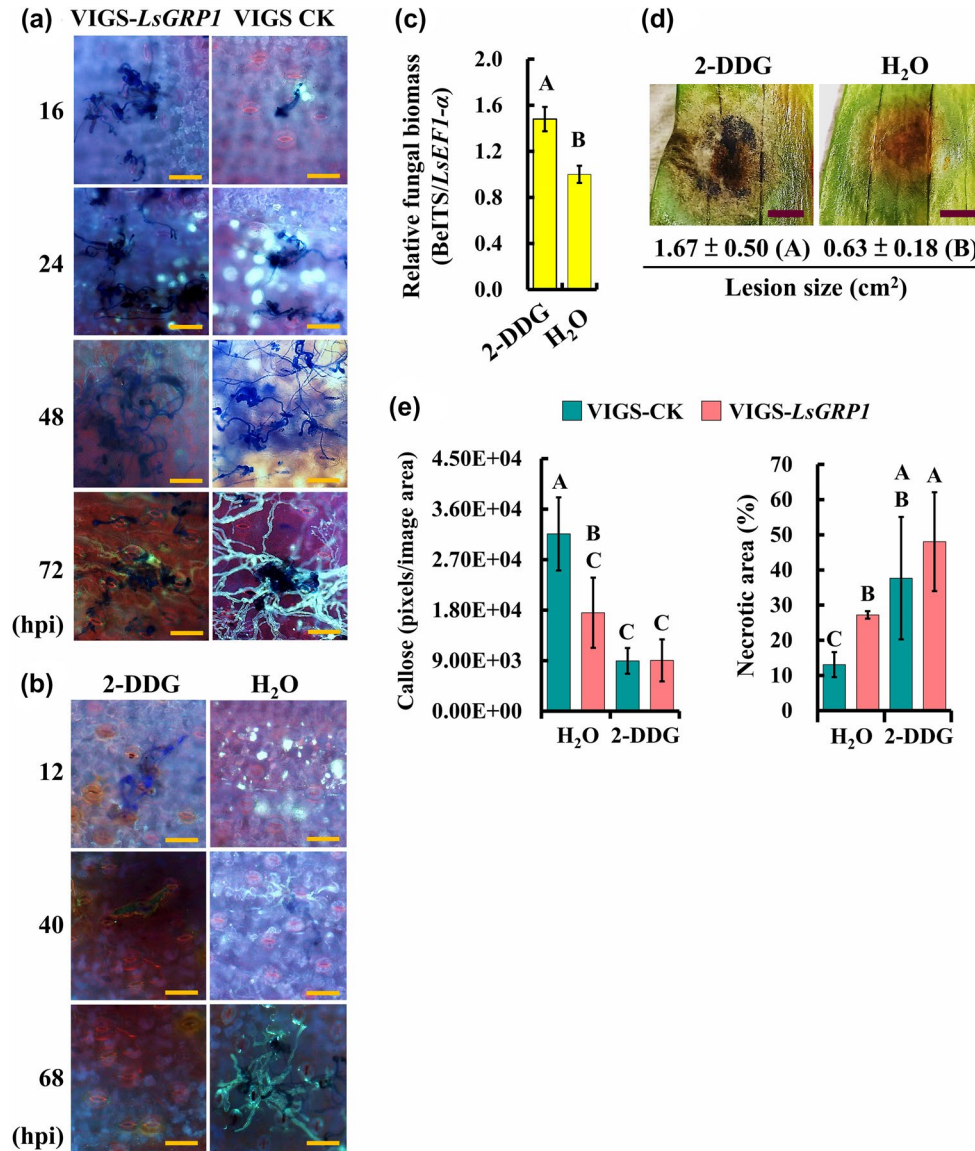
FIGURE 2 *LsGRP1*-enhanced callose deposition suppresses *Botrytis elliptica* infection in lily. (a) *LsGRP1* silencing reduced callose deposition in response to *B. elliptica* challenge. *LsGRP1*-silenced (VIGS-*LsGRP1*) and VIGS-control (VIGS-CK) leaves were droplet-inoculated with a 20-μl spore suspension of *B. elliptica* at 5×10^4 spores/ml. Callose deposition and fungal growth were visualized by aniline blue and trypan blue double staining. hpi, hours post-inoculation. (b)–(d) Inhibition of callose deposition in lily enhanced *B. elliptica* infection and symptom development. Lily leaves were droplet-inoculated with a 20-μl spore suspension of *B. elliptica* at 5×10^4 spores/ml at 28 hr after infiltration with 1 mM 2-deoxy-D-glucose (2-DDG, a callose synthesis inhibitor) or sterile deionized water (H_2O). (b) Effect of callose inhibitor on callose deposition and in planta fungal growth visualized by aniline blue and trypan blue double staining. (c) Relative *B. elliptica* biomass at 68 hpi detected by quantitative PCR. (d) Symptoms at 7 days post-inoculation (dpi). (e) The treatment of 2-DDG reduced LsGRP1-conferred grey mould resistance. Lily leaves were spray-inoculated with *B. elliptica* at 5×10^4 spores/ml at 28 hr after 2-DDG infiltration. Callose deposition and necrotic lesions were detected and quantified at 16 hpi and 3 dpi after aniline blue and trypan blue staining, respectively. Data represent the mean $\pm$ *SD* from three, three, and five biological replicates in (c), (d), and (e), respectively. Statistical analysis was performed using analysis of variance followed by LSD test ($p < .05$). Bar: 100 μm in (a) and (b); 0.5 cm in (d)

PCD-inducing efficiencies throughout the whole observation period rather than SUMO-LsGRP1ΔC, SUMO-CK, and sterile deionized water treatments, which all failed to induce fungal apoptosis PCD at early (24 hpi) and late (96 hpi) infection stages. Therefore, the fungal apoptosis PCD-inducing activity of LsGRP1 conferred by antimicrobial LsGRP1[C] region involved in lily resistance against grey mould is presumed.

2.4 | *LsGRP1*-transgenic *Arabidopsis* exhibits enhanced resistance to necrotrophic and hemibiotrophic pathogens accompanied with enhanced defence responses

LsGRP1 driven by a constitutive 2×35S promoter was introduced into the dicot model *Arabidopsis thaliana* accession Columbia-0
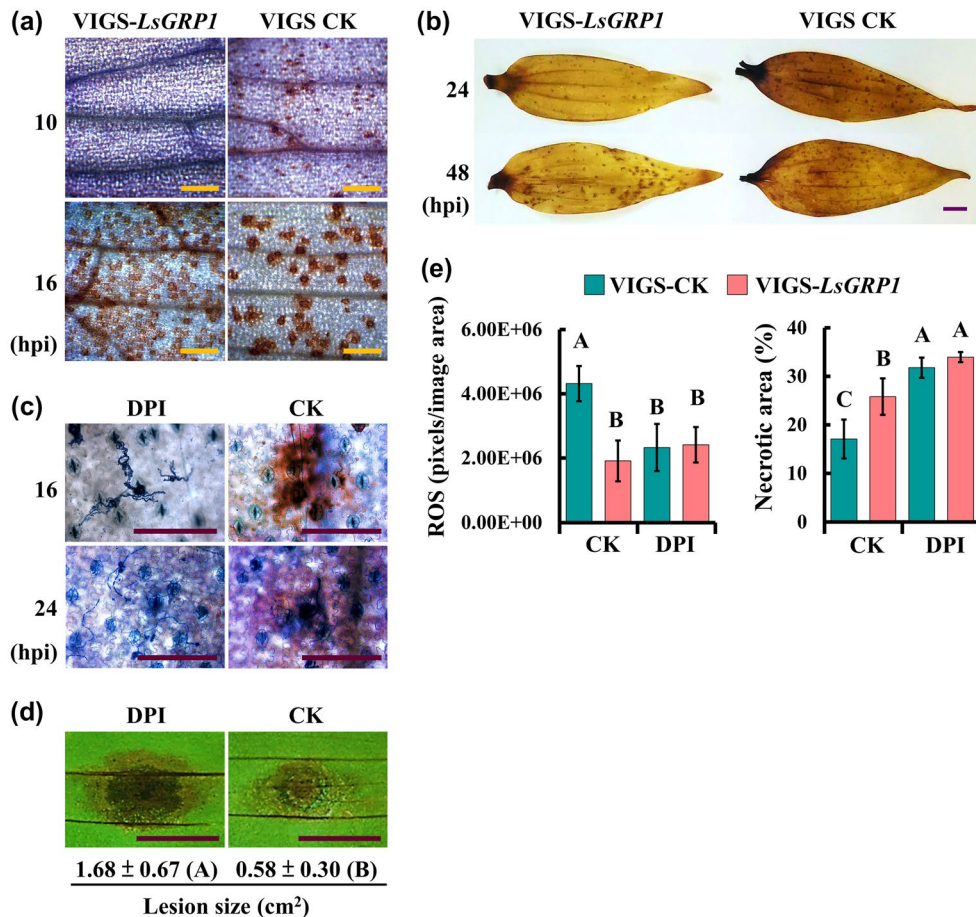
FIGURE 3 *LsGRP1*-tiggered early accumulation of reactive oxygen species (ROS) is required for grey mould resistance of lily. (a) and (b) *LsGRP1* silencing delayed ROS accumulation. *LsGRP1*-silenced (VIGS-*LsGRP1*) and VIGS-control (VIGS-CK) leaves were spray-inoculated with a spore suspension of *B. elliptica* at 5 × 10⁴ spores/ml. The micro- (a) and macro-views (b) of ROS accumulation were observed after 3,3′-diaminobenzidine (DAB) staining. (c) and (d) Inhibition of ROS generation enhanced grey mould susceptibility of lily. Lily leaves were droplet-inoculated with a 20-μl spore suspension of *B. elliptica* at 5 × 10⁴ spores/ml at 1 hr after infiltration with 100 μM diphenyleneiodonium (DPI, a ROS generation inhibitor, prepared in 1% DMSO) or 1% DMSO (CK). (c) ROS accumulation and fungal growth/plant cell death visualized by DAB and trypan blue double staining. (d) Lesion size at 4 days post-inoculation (dpi). (e) The treatment of DPI reduced LsGRP1-conferred grey mould resistance. Lily leaves were spray-inoculated with *B. elliptica* at 5 × 10⁴ spores/ml at 1 hr after DPI infiltration. ROS accumulation and necrotic lesions were detected and quantified at 16 hpi and 3 dpi after DAB and trypan blue staining, respectively. Data represent the mean ± SD from five and four biological replicates in (d) and (e), respectively. Statistical analysis was performed using analysis of variance followed by LSD test (*p* < .05). Bar: 25 μm in (a) and (c); 1 cm in (b) and (d)

(Col-0) (Figure S2) to examine its effect on disease suppression against necrotrophic and hemibiotrophic pathogens as well as defence enhancement. Under standard growth conditions, the T₅ generation of self-pollinated, homogeneous *LsGRP1*-transgenic lines (LsGRP1-2 and LsGRP1-7) grew like the wild-type (WT) *Arabidopsis* (Figure 6a) and reproduce normally, suggesting that *LsGRP1* expression in the absence of pathogen challenge did not directly launch plant defence, which generally antagonizes growth. When challenged withthe necrotrophic fungus *B. cinerea*, *LsGRP1*-transgenic lines developed much milder symptoms (Figure 6b). Histochemical staining assays at 1 dpi indicated that spore germination and hyphal growth of *B. cinerea* were obviously inhibited in *LsGRP1*-transgenic lines, accompanied with the callose-deposited papilla formed in front of hyphal tips. By contrast, the papillae were passed through by fungal hyphae in WT *Arabidopsis*. Likewise, ROS

accumulated more in *LsGRP1*-transgenic lines than WT *Arabidopsis*. The relative amounts of callose and ROS in *LsGRP1*-transgenic lines at 1 dpi were measured to be approximately 9.0-fold and 1.6-fold higher than those in WT *Arabidopsis*, respectively (Figure 6c). In addition, the TUNEL assay showed that *B. cinerea* mainly underwent hyphal apoptosis PCD at 2 dpi in WT *Arabidopsis*, consistent with the previous report by Shlezinger *et al.* (2011a,2011b); however, it underwent spore apoptosis PCD at 1 dpi and hyphal apoptosis PCD at 2 dpi in *LsGRP1*-transgenic lines (Figure 6d), demonstrating that *LsGRP1* expression in *Arabidopsis* accelerated the occurrence of host-induced apoptosis PCD in *B. cinerea*. In terms of challenge with the hemibiotrophic bacterium *Pseudomonas syringae* pv. *tomato* (Pst DC3000), *LsGRP1*-transgenic lines clearly reduced symptom development and bacterial population growth as compared to WT *Arabidopsis* (Figure 6e). Stronger callose deposition and ROS
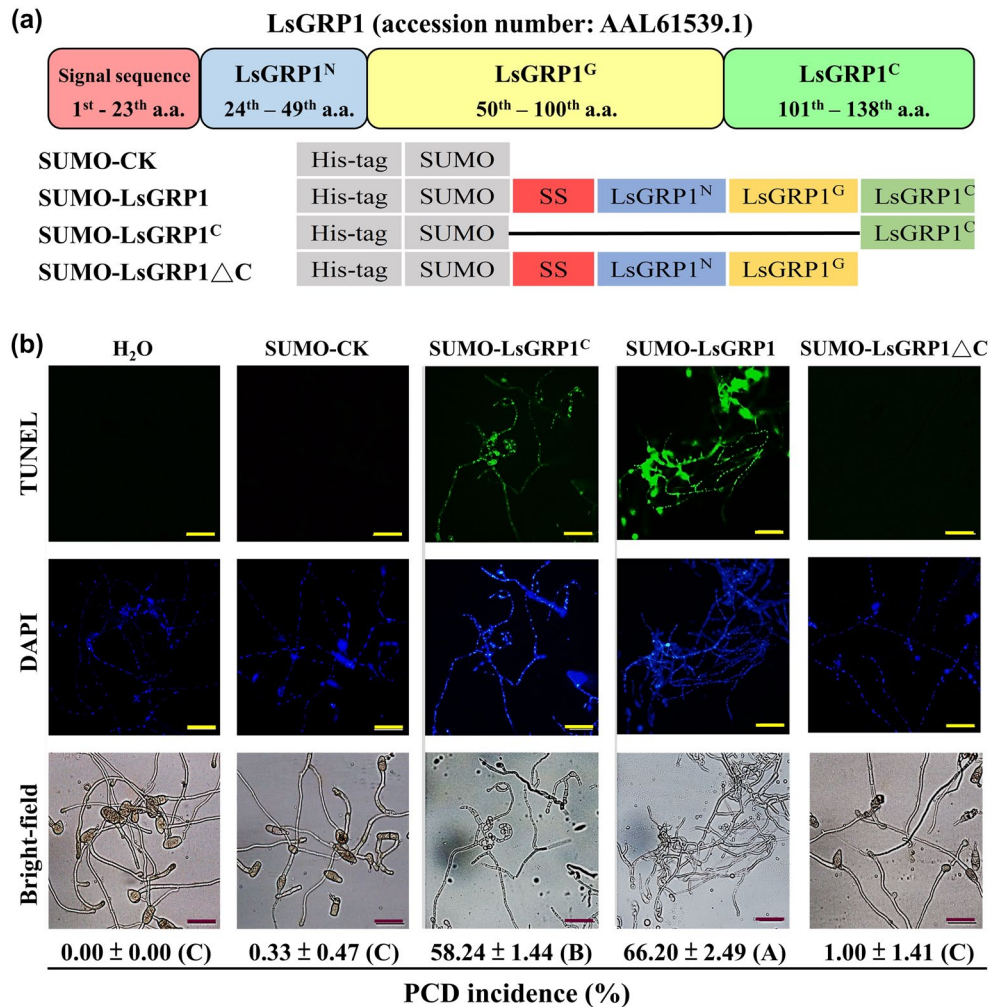
FIGURE 4 LsGRP1^C plays an essential role in LsGRP1-inducing fungal apoptosis programmed cell death (PCD). (a) Schematic diagram of LsGRP1-derived recombinant proteins and the recombination partner SUMO-CK. (b) The hyphae of *Botrytis elliptica* were treated with a 10 μM solution of each protein for 24 hr. Total fungal nuclei and the nuclei undergoing chromosomal DNA fragmentation were detected by 4′,6′-diamidino-2-phenylindole (DAPI) staining and a terminal deoxynucleotidyl transferase dUTP nick end-labelling (TUNEL) assay, respectively. Sterile deionized water (H$_2$O) was used instead of protein solutions as a negative control. The incidence rate of fungal apoptosis PCD was calculated based on the ratio of TUNEL-labelled nuclei to DAPI-labelled nuclei. Data represent the mean $\pm$ *SD* of three biological replicates and subjected to analysis of variance followed by LSD test ($p < .05$). Different upper case letters in parentheses indicate significant differences. Bar: 50 μm

accumulation against Pst DC3000 were also indicated in *LsGRP1*-transgenic lines by histochemical staining and subsequent signal quantification (Figure 6f). These results revealed that LsGRP1 consistently mediates defence activation to defeat pathogens of different infection and nutrition modes as well as induces fungal apoptosis PCD in the dicot *Arabidopsis* as in the monocot *Lilium*.

2.5 | *LsGRP1* contributes to lily vitality against host-killing secretion of *B. elliptica* and pathogen-triggered innate immune activation

Necrotrophic fungal secretion, which contains toxins, cell wall-degrading enzymes, effectors, PAMPs, and small RNAs, can activate or suppress plant immunity (Wang *et al.*, 2014). Lily cell death induced

by *B. elliptica* secretion is essential for the subsequent infection of lily by compatible and even incompatible *Botrytis* species (van Baarlen *et al.*, 2004). Accordingly, the effects of *LsGRP1* expression on lily vitality and defence activation in response to *B. elliptica* secretion and PAMP treatments were surveyed. While *LsGRP1* was silenced, lily leaf cell death caused by preinfiltration with *B. elliptica* secretion became more severe accompanied with the reduction of callose deposition, which were indicated by conductivity measurement and aniline blue staining, respectively (Figure 7a,b). The levels of PTI-associated callose deposition elicited by PAMP treatments of bacterial flg22 and fungal chitohexaose 1 day after treatment were also clearly decreased in *LsGRP1*-silenced lily (Figure 7c). These findings revealed that LsGRP1 contributes to the survival of leaf tissue from the necrosis-inducing *B. elliptica* secretion and the PTI activation in lily.

FIGURE 5 Increasing LsGRP1[C] abundance in leaves promotes grey mould resistance of lily by enhancing fungal apoptosis programmed cell death (PCD). Lily leaf disks were infiltrated with 10 µM protein solution of SUMO-LsGRP1[C], SUMO-LsGRP1, SUMO-LsGRP1ΔC, or control protein of SUMO fusion partner (SUMO-CK) and droplet-inoculated with a 10-µl spore suspension of *Botrytis elliptica* at 5×10^4 spores/ml 1 hr later. Relative biomass (a) and in planta growth (b) of *B. elliptica* were detected by quantitative PCR and trypan blue staining, respectively, at 24 hours post-inoculation (hpi). (c) Total fungal nuclei and the nuclei undergoing chromosomal DNA fragmentation were detected by 4′,6′-diamidino-2-phenylindole (DAPI) staining and terminal deoxynucleotidyl transferase dUTP nick end-labelling (TUNEL) staining, respectively. (d) The incidence rate of fungal apoptosis PCD was calculated based on the ratio of TUNEL-labelled nuclei to DAPI-labelled nuclei. Sterile deionized water (H₂O) was used instead of protein solutions as a negative control. Data represent the mean ± *SD* of three biological replicates. Statistics analysis was performed using analysis of variance followed by LSD test ($p < .05$). Bar: 100 µm in (b); 25 µm in (c)
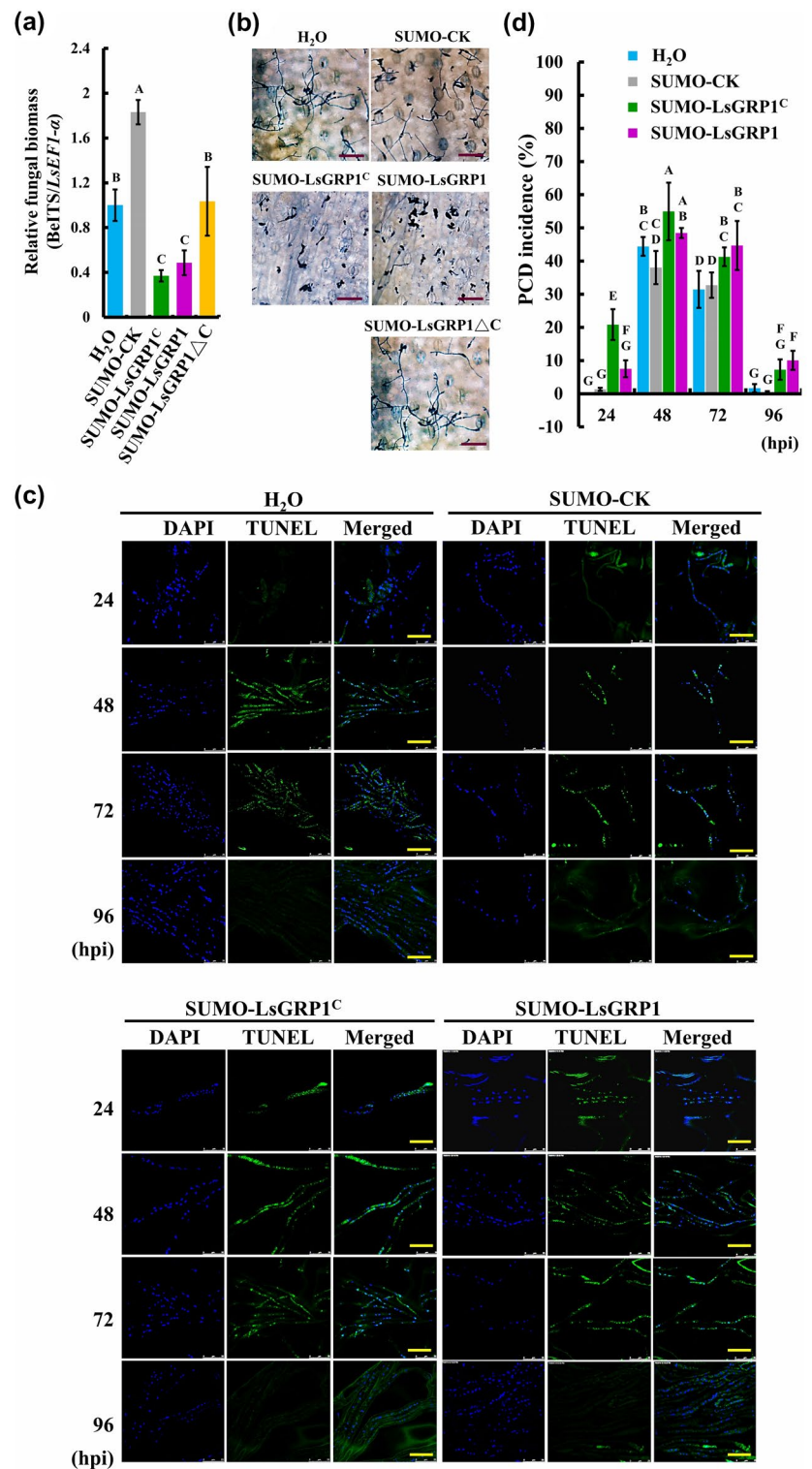
The involvement of LsGRP1 in activating PTI and ETI, two major branches of innate immune system, was further demonstrated using *LsGRP1*-transgenic *Arabidopsis*. In terms of PTI activation, histochemical staining assays and subsequent signal quantification revealed that both callose deposition and ROS accumulation in response to flg22 and chitohexaose treatments were obviously increased in *LsGRP1*-transgenic lines as compared to WT *Arabidopsis* (Figure 8a,b). Also, PAMP-induced *AtrbohD* expression required for PTI-associated ROS generation (Bigeard *et al.*, 2015; Peng *et al.*, 2018) was more greatly up-regulated in *LsGRP1*-transgenic lines as evaluated by RT-qPCR (Figure 8c). In terms of ETI activation, HR elicitation from the recognition of AvrRpm1 and AvrRpt2 effectors by the corresponding R proteins present in *Arabidopsis* accession Col-0 was significantly enhanced by *LsGRP1* expression as detected by an Evans blue staining-based quantification method (Figure 8d). By contrast, leaf cell death seldom occurred in

both WT and *LsGRP1*-transgenic *Arabidopsis* after agroinfiltration with empty vector control (EV) or AvrPto effector, which could not be recognized by *Arabidopsis* accession Col-0. As a consequence, LsGRP1 acting downstream of R protein–effector recognition to boost the ETI-associated HR was presumed. According to these findings, it was concluded that *LsGRP1* contributes to PTI and ETI activation as well as the antinecrotic activity against the necrotrophic fungus.

3 | DISCUSSION

Although many monocot species are reported to exhibit induced resistance by the treatments of certain plant defence activators and beneficial rhizosphere microorganisms, the underlying regulatory mechanism of the induced defence, particularly in noncereals, is not clear yet (Balmer *et al.*, 2013). In this study, SA-induced LsGRP1 of lily is demonstrated to trigger innate immune activation in response

FIGURE 6 *LsGRP1* expression increases *Arabidopsis* resistance against the necrotrophic *Botrytis cinerea* and the hemibiotrophic *Pseudomonas syringae* pv. *tomato* DC3000 by enhancing LsGRP1-related defence responses. (a) Morphology of 24-day-old wild-type (WT) *Arabidopsis thaliana* accession Col-0 and the T_5 generation of self-pollinated, homogeneous *LsGRP1*-transgenic lines (LsGRP1-1 and LsGRP1-7). The rosette leaves were spray- (b) or droplet-inoculated (10 μl in [b], [c], and [d]) with spore suspension of *B. cinerea* at 5×10^5 spores/ml, or spray (left panel of [e]) or infiltrated (right panel of [e] and [f]) with bacterial suspension of *P. syringae* pv. *tomato* DC3000 at 1.5×10^8 (left panel of [e]), 1.5×10^6 (right panel of [e]) or 1.5×10^7 cfu/ml (f). (b) Trypan blue-stained necrotic lesions and symptom at 2 and 3 days post-inoculation (dpi), respectively. The sizes of necrosis lesions caused by droplet-inoculation were quantified. (c) Callose deposition, reactive oxygen species (ROS) accumulation, and *B. cinerea* growth detected by aniline blue, 3,3′-diaminobenzidine (DAB), and trypan blue staining, respectively, at 1 dpi. (d) Fungal apoptosis programmed cell death (PCD) visualized by terminal deoxynucleotidyl transferase dUTP nick end-labelling (TUNEL) staining. Pink and blue arrows indicate the spores and hyphal cells undergoing apoptosis PCD, respectively. (e) Symptom and bacterial population at 5 dpi. (f) Callose deposition and ROS accumulation detected and quantified after aniline blue staining and DAB staining, respectively. Bar: 100 μm in (c); 200 μm in (d); 400 μm in (f). Data represent the mean ± *SD* of five, six, three, and six biological replicates in (b), (c), (e), and (f), respectively. Statistics analysis was performed using analysis of variance followed by LSD test ($p < .05$). Significant differences in (b) are indicated by different uppercase letters in parentheses
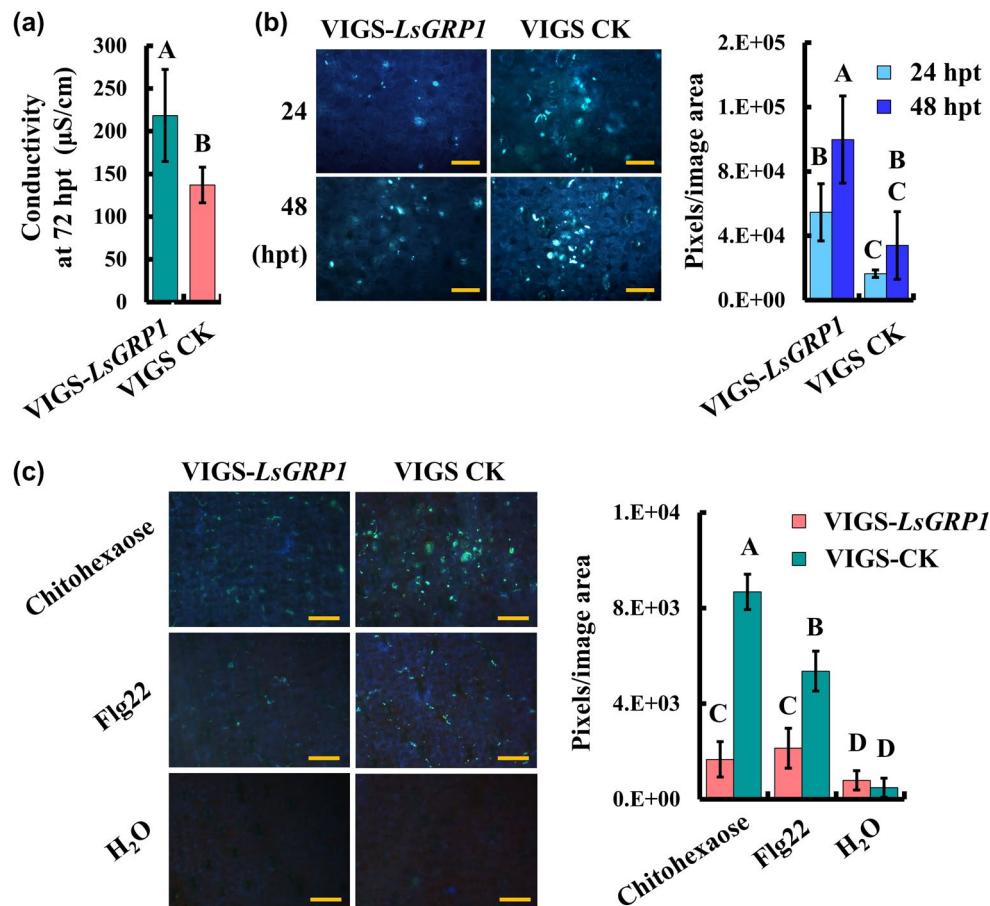

FIGURE 7 *LsGRP1* confers anti-cell death activity against *Botrytis elliptica* secretion and involves PAMP-triggered immunity of lily. Leaf discs of *LsGRP1*-silenced (VIGS-*LsGRP1*) and VIGS-control (VIGS-CK) lily plants were infiltrated with *B. elliptica* secretion ([a] and [b]) or PAMP solutions of 1 μM flg22 or 10 μM chitohexaose (b). The relative levels of cell death (a) and callose deposition ([b] and [c]) were detected by conductivity measurement and aniline blue staining, respectively. Data represent the mean ± *SD* of five biological replicates. Statistical analysis was performed using analysis of variance followed by LSD test ($p < .05$). hpt, hours post-treatment. Bar: 100 μm in (b) and (c)

to the appearance of pathogenic stimulators, including PAMPs and very probably effectors that would be present in *B. elliptica* secretion. It is worth noting that LsGRP1 promotes lily shoot elongation and reduces *B. elliptica* secretion-induced lily apoptosis PCD, which is essential for the subsequent *Botrytis* infection (van Baarlen *et al.*, 2004), indicating its involvement in manipulating plant physiology and resistance to *Botrytis*. In addition, LsGRP1 enables the apoptosis PCD of *B. elliptica* in lily via the antimicrobial C-terminal region

LsGRP1[C], an event similar to camalexin-triggered apoptosis PCD of *B. cinerea* in *Arabidopsis* (Shlezinger *et al.*, 2011a, 2011b; Veloso and van Kan, 2018). This finding reveals that host-induced fungal apoptosis PCD may be a common defence mechanism against necrotrophic fungi or at least *Botrytis* spp. The dual function of LsGRP1 in innate immune activation and fungal apoptosis PCD induction is also shown in *Arabidopsis* to improve the resistance to both necrotrophic and hemibiotrophic pathogens. For the first time, a plant class II GRP
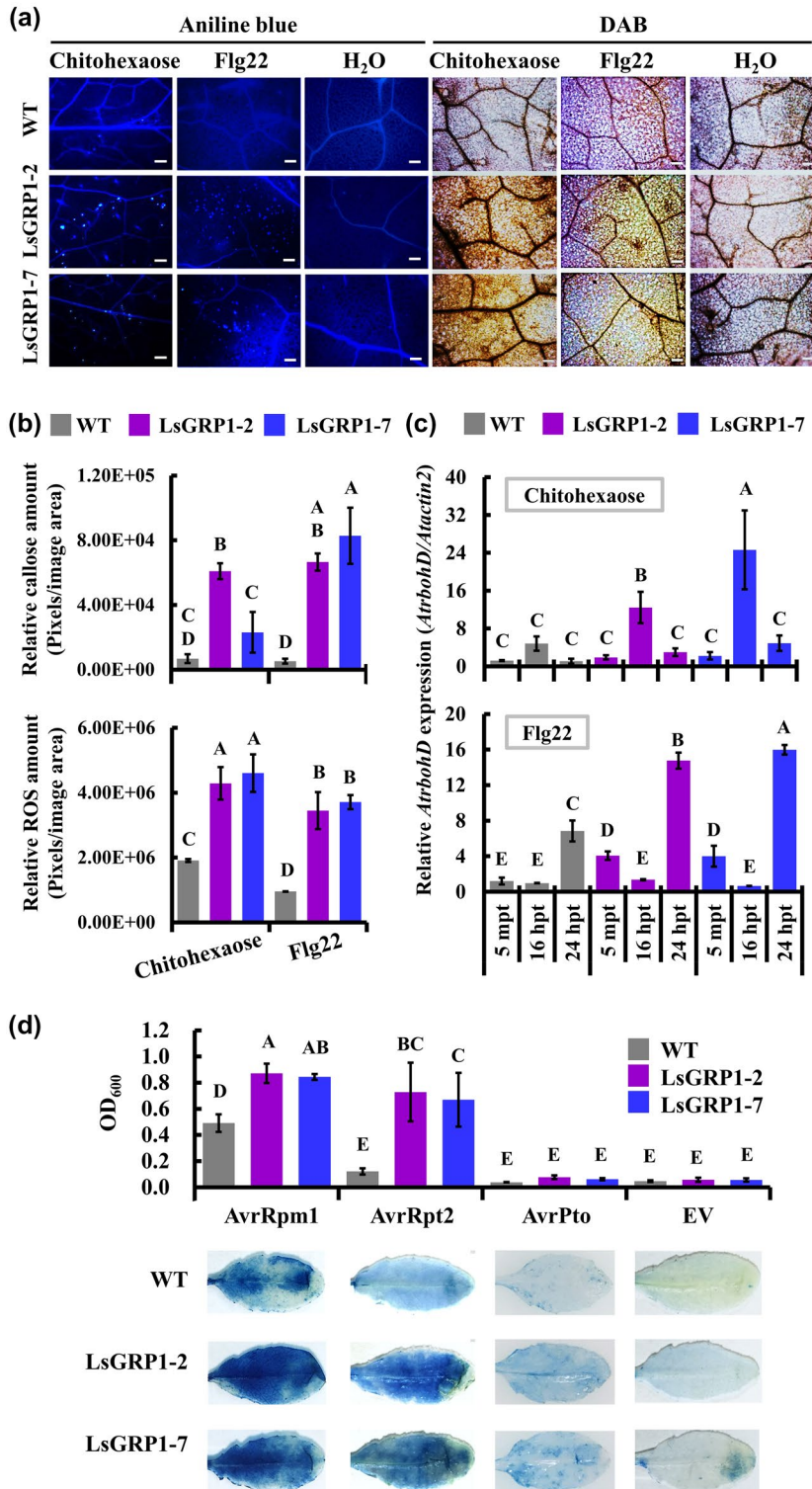
(a)

FIGURE 8 *LsGRP1* expression boosts the activation of innate immune responses in *Arabidopsis*. Rosette leaves of wild-type (WT) *Arabidopsis* and *LsGRP1*-transgenic lines (LsGRP1-1 and LsGRP1-7) were infiltrated with 1 μM flg22 or 10 μM chitohexaose. PAMP perception-induced callose deposition and reactive oxygen species (ROS) accumulation in treated leaves were detected 24 hr later by aniline blue and 3,3′-diaminobenzidine (DAB) staining, respectively (a). The relative amounts of callose and ROS in (a) were quantified (b). The relative expression of *AtrbohD* was compared by quantitative reverse transcription PCR (c). Sterile deionized water (H₂O) was used as a negative control. mpt, minutes post-treatment; hpt, hours post-treatment. Bar: 100 μm. The rosette leaves of *Arabidopsis* were agroinfiltrated with AvrRpm1, AvrRpt2, or AvrPto effectors of *Pseudomonas syringae*. Effector recognition-induced hypersensitive response in agroinfiltrated leaves were estimated by the Evans blue staining-based quantification method 2 days later (d). EV, empty vector control of agroinfiltration. Data represent the mean ± *SD* of four biological replicates. Statistical analysis was performed using analysis of variance followed by LSD test (*p* < .05)

is proven to trigger in planta fungal apoptosis PCD and mediate the induced defence mechanism seemingly implicated with growth–defence trade-offs in lily, which is perhaps highly employed in monocot species and has a consistent effect on dicot species.

Plant genes involved in defence priming generally cause alterations crucial for the enhanced defensive behaviour instead of directly triggering defence responses that antagonize growth in the absence of pathogens (Mauch-Mani *et al.*, 2017). Because LsGRP1

enabled a faster and stronger defence in response to pathogenic stimulators in both lily and *Arabidopsis*, and the overexpression of *LsGRP1* by a very strong constitutive 2×35S promoter did not obviously affect *Arabidopsis* growth and reproduction under unchallenged conditions, the function of LsGRP1 in defence priming is presumed. However, *LsGRP1* silencing unexpectedly caused a minor reduction in lily shoot length. It is known that *LsGRP1* expression in lily is maintained at a basal level under unchallenged

conditions and is induced to higher levels by *B. elliptica* challenge and the treatments of defence activator SA and probenazole, which all trigger enhanced resistance to grey mould (Lu and Chen,1998, 2005; Chen *et al*., 2003; Lu *et al*., 2007; Lin and Chen,2014, 2017). Consistent with this,the *LsGRP1* promoter exhibits a basal activity and can be activated by stresses and defence hormone treatments, especially pathogen attacks, in lily and *Nicotiana tabacum*. In addition, the multiple light-responsive and mesophyll expression-related regulatory elements present inthe *LsGRP1* promoter coincide with the leaf-specific accumulation of LsGRP1 (Lin and Chen,2014, 2017). The application of 3-(3,4-dichlorophenyl)-1,1-dimethylurea, a photosynthesis inhibitor, suppresses the expression of *LfGRP1*, a *LsGRP1* homolog from *Lilium formosanum* (Liu *et al*., 2010), implying a photosynthesis-dependent manner of *LsGRP1* expression. To summarize, the basal accumulation of LsGRP1 in lily leaves is regarded not only to sustain the timely defence induction in response to pathogens but possibly promote plant growth, which may be involved in photosynthesis. The growth-promoting function of LsGRP1 can be further clarified using *LsGRP1*-transgenic *Arabidopsis*. As some LsGRP1-interacting proteins were previously isolated from lily leaf tissues via co-immunoprecipitation (Lin and Chen, 2014), the identification and characterization of these proteins would help to uncover the underlying mechanism.

The enormous and timely increases of ROS and antioxidant activities were supposed to be the main contributors to the high grey mould resistance of Oriental hybrid *Lilium* cultivar Sorbonne (Gao *et al*., 2018). In this study, the rapid and intense ROS accumulation and callose deposition at *B. elliptica* attacking sites were first demonstrated to exhibit great inhibitory effects against *B. elliptica* infection, indicating that these two PTI-associated defence responses mainly mediated by LsGRP1 are necessary to grey mould resistance of lily. Besides, *AtrbohD* expression required for PTI-associated ROS generation in *Arabidopsis* (Bigeard *et al*., 2015; Peng *et al*., 2018) had higher induction levels in *LsGRP1*-transgenic lines compared to WT *Arabidopsis* at 5 min and 24 hr after PAMP treatments, also providing transcriptional evidence that *LsGRP1* expression enables a stronger ROS accumulation soon after pathogen attacks. By contrast, grey mould-susceptible *LsGRP1*-silenced *Lilium* cultivar Stargazer did not accumulate large amounts of ROS until 48 hpi, by when the grey mould-resistant lilies were reducing ROS amounts (refer to Gao *et al*., 2018; this study). Small oxidative bursts act as secondary messengers of various signalling pathways, including defence pathways, and are often important for the initiation and spread of HR, a unique PCD in plants. However, excess ROS accumulation can guide plant cells to commit suicide through apoptosis, which is a type of PCD favoured by certain necrotrophic pathogens feeding on dead host cells, such as *B. cinerea* (Veloso and van Kan, 2018; Balint-Kurti, 2019; Lorang, 2019). In addition, *B. elliptica* secretion-induced lily cell death belongs to apoptosis, which is required for the subsequent fungal infection (van Baarlen *et al*., 2004). Recently, the dynamic equilibrium between two types of PCD, that is, the mutually antagonistic autophagy and apoptosis, was regarded as determining the plant trends to grey mould resistance and susceptibility, respectively. As is known, low levels of

cellular ROS induce autophagy, a mechanism to restore cellular homeostasis, whereas excess ROS accumulation brings out apoptosis, which occurs in cells undergoing an irrecoverable traumatic event or cellular remodelling (Cooper, 2018; Veloso and van Kan, 2018). Taken together, plant HR and *B. elliptica* secretion-induced lily cell death both belong to PCD (van Baarlen *et al*., 2004; Balint-Kurti, 2019), and have higher occurrence in grey mould-resistant and susceptible lilies, respectively, based on our observations. We presume the former one was autophagy, which is elicited by the rapid and intense ROS accumulation triggered by effective pathogen recognition, but the later one was apoptosis, which should result from excess ROS accumulation implicated with severe *B. elliptica* infection and might be classified as, or mixed up with, necrotic cell death traditionally. LsGRP1 may adjust the occurrence timing and types of lily PCD via mediating a finely tuned balance of ROS accumulation soon after pathogen attack to promote grey mould resistance. It should also be considered that HR in lily may be beneficial for *B. elliptica* infection. Further assays with the inducers, inhibitors, or mutants of autophagy and apoptosis would help to verify this assumption.

B. elliptica inocula at 5 and 10×10^4 spores/ml have over 80% spore germination rates, and 54.5% and 62.0% penetration rates, respectively, in leaves of Stargazer lily at 12 dpi as directly observed under light microscopy (Hsieh *et al*., 2001; Hou and Chen, 2003). However, our histochemical detection of callose showed few spores and numerous callose deposition sites in the leaves of water treatment at 12 hpi (Figure 2b), which may be because most non-penetrating and slightly penetrating spores had been removed after the histochemical staining procedure. The deposition of callose, $(1,3)$-β-glucan, between the plasma membrane and cell wall acts as a physical barrier to prevent or delay pathogen invasion. Callose-rich papillae, comprising mainly callose and other cell wall polymers, phenolic compounds, ROS, antimicrobial compounds, and cell wall proteins, are regarded as a ubiquitous defence response associated with penetration resistance. The timing of callose deposition and papillae formation at pathogen attack sites could be the key parameter for optimal effectiveness against infection (Ellinger and Voigt, 2014; Voigt, 2014). In addiiton, an effective papilla is hypothesized to have a higher ROS content and particular cell wall polymer composition (Hückelhoven, 2014). Herein, the rapid and intense ROS accumulation at pathogen attack sites mediated by LsGRP1 may contribute to the timing and effectiveness of callose deposition and papilla formation against pathogen invasion. Intriguingly, whether the plasma membrane- and cell wall-localized LsGRP1 also abundantly accumulates in these callose and papillae and acts collaboratively to inhibit pathogens by its antimicrobial LsGRP1^C region (Lin *et al*., 2014, 2017) should be taken into consideration and further investigated.

B. cinerea infection of *Arabidopsis* is impeded by camalexin-induced hyphal apoptosis PCD until part of the hyphal cells escape from this host defence machinery by the action of the anti-apoptotic protein BcBIR1 (Shlezinger *et al*., 2011a,b; Veloso and van Kan, 2018). The camalexin-deficient *pad3* mutant is fully susceptible not only to *B. cinerea* but also to incompatible *B. elliptica* and *Botrytis tulipae*, a tulip-specific pathogen (van Baarlen *et al*., 2007).

Like camalexin, LsGRP1 triggers the apoptosis PCD of *B. elliptica* in lily and accelerates the apoptosis PCD of *B. cinerea* in *Arabidopsis*, which is contributed from its fungal apoptosis PCD-inducing region LsGRP1[C] (Lin *et al.*, 2014, 2017; this study). Herein, the pathogenicity and virulence of *Botrytis* species could be at least partially defined by their resistance to fungal apoptosis PCD inducers of plants. It is worth noting, with reference to LsGRP1-conferring grey mould resistance, that the compatibility between plants and *Botrytis* species would be also reduced by the innate immune activation mediated by LsGRP1.

The C-terminal region of LsGRP1 is the first case of class II GRPs found to function as a fungal apoptosis PCD-inducing domain to assist disease resistance (Lin and Chen, 2014, 2017; this study). By contrast, AtGRP3 and CpGRP1 use the C-terminal regions to interact with cell wall-associated kinases (WAKs), and thereby affect disease resistance and probably dehydration-related responses, respectively (Park *et al.*, 2001; Yang *et al.*, 2003; Giarola *et al.*, 2016; Gramegna *et al.*, 2016; Jung *et al.*, 2019). As the C-terminal regions of plant class II GRPs share higher sequence similarities with the others belonging to the same clades of either monocot or dicot (Figure S3), the antimicrobial activity associated with most or certain C-terminal regions of class II GRPs is of interest to investigate. In contrast, some WAKs are known to confer broad-spectrum as well as pathogen race-specific resistances, or exhibit an evolved ability to recognize DAMP oligogalacturonides, which generally result from cell wall digestion by the secreted cell wall-degrading enzymes of necrotrophic fungi (Wang *et al.*, 2014; Bacete *et al.*, 2018; Kanyuka and Rudd, 2019). The dramatic expansion of WAK families in maize and wheat implies a particular importance of WAKs in the immunity of monocot species (Kanyuka and Rudd, 2019). Because LsGRP1 also has some interactors in lily leaves (Lin and Chen, 2014) and enables the enhanced defence activation of lily and *Arabidopsis*, LsGRP1 may play a role in the immunity of different plant species through interacting with their WAKs. In addition, because *B. elliptica* secretion was seemingly superior to PAMP flg22 and chitohexaose in triggering callose deposition in lily, the lower sensitivity of lily PRRs to these PAMPs and the differential preference for PAMPs between lily and model dicot species are presumed. Host recognition of some other molecular patterns or a combination of these molecules may be required for a strong innate immune activation mediated by LsGRP1 in lily.

LsGRP1 originates from *Lilium* cultivar Stargazer belonging to Oriental hybrids, the horticultural division 7, which mainly comprises the crossbreeds derived from *Lilium auratum* and *Lilium speciosum*, including cultivar Stargazer, and some other crossbreeds within *Lilium* section *Archelirion* (McRae, 1998; van Tuyl and Arens, 2011). Cultivar Stargazer, the first Oriental hybrid with up-facing blooms bred by Leslie Woodriff in the 1970s, was the most popular lily cultivar for over 25 years and has served as an important parent cultivar for lily breeding (van Tuyl and Arens, 2011). Because the Oriental hybrids appear less vulnerable to grey mould compared to the other divisions (Balode and Belicka, 2004; Daughtrey and Bridgen, 2013; Gao *et al.*, 2018), it is presumed that LsGRP1 or its homologs are commonly present in Oriental hybrids, and thus result in the higher grey mould resistance. In addition, *LfGRP1*, a *LsGRP1* homolog of *L. formosanum* belonging to division 9, shares a similar expression profile with *LsGRP1* under the challenge of *B. elliptica* or the treatment of systemic resistance-eliciting rhizobacteria (Liu *et al.*, 2008). Accordingly, the presence, sequence similarity, and expression profile of LsGRP1 homologs can be surveyed in lily species and cultivars that exhibit different levels of grey mould resistance to clarify the general relationship between LsGRP1 homologs and grey mould resistance in *Lilium* plants. This investigation would provide the foundation for the use of *LsGRP1* as a grey mould-resistance marker or a resource for lily breeding and improve the exploration of novel defence genes and defence mechanisms in lily.

In this study, the TRV ratio in TRV vector-treated and untreated Stargazer lily plants was determined to be approximately 3:1 by RT-qPCR. The high C_t values (over 30) of different TRV targets, including the genes of viral replicase and movement protein in RNA1 and coat protein in RNA2, were generally found in our silencing assays of *LsGRP1* and other genes of Stargazer lily (unpublished), which means that even a very small amount of in planta TRV vector enables efficient gene silencing in Stargazer lily. In addiiton, TRV infection may occur in bulbs of Stargazer lily and it also presents in another lily cultivar, Sorbonne (Jo and Cho, 2018). Although the TRV vector can also silence the *PDS* gene of *Lilium* × *formolongi*, the TRV titre was not reported (Xu *et al.*, 2019). It would be interesting to determine the relationship between gene silencing efficiency and TRV vector titre in different *Lilium* plants.

This study found that LsGRP1 exhibits a dual function in plant defence, which involves innate immune activation and fungal apoptosis PCD induction, to protect plants from necrotrophic and hemibiotrophic pathogens. Accordingly, a class II GRP, like LsGRP1, could serve as a potential entry point to expound the immune mechanisms of monocot species, especially noncereals, and as a promising breeding resource due to its compatibility in crop production and protection of both monocots and dicots.

4 | EXPERIMENTAL PROCEDURES

4.1 | Plant materials

The bulbs of Oriental hybrid *Lilium* cultivar Stargazer with a circumference of 16–18 cm were planted in a potting mix containing BVB Substrate No. 2 (Bas van Buuren), vermiculite and perlite at a ratio of 6:1:1 (vol/vol/vol) and cultured at 18–20°C for 7–9 weeks under a light/dark cycle of 16/8 hr. The seeds of *A. thaliana* accession Col-0 and its derived transformants were sown in the same potting mixture and cultured at 23–27°C for 3–4 weeks under a light/dark cycle of 16/8 hr.

4.2 | Pathogen inoculation and quantification

B. elliptica strain B061 was cultured on V8 medium (20% V8 vegetable juice [Campbell Soup Co.], 0.3% $CaCO_3$, 1.5% agar) at 18–20°C

for 5–7 days for sporulation. The conidial spores were suspended in 0.05% Tween-20 solution and adjusted to a final concentration of 5×10^4 spores/ml. *B. cinerea* strain W2 was cultured on potato dextrose agar (Difco Laboratories Inc.) at 23–27 °C for 10–14 days for sporulation. The conidial spores were suspended in 0.5 × potato dextrose broth (Difco Laboratories Inc.) and adjusted to a final concentration of 5×10^5 spores/ml. The middle leaves of lily and the rosette leaves of *Arabidopsis* were challenged with the spore suspensions of *B. elliptica* and *B. cinerea*, respectively, by droplet- or spray-inoculation and kept moist under plant growth conditions until assay. *P. syringae* pv. *tomato* DC3000 was inoculated into Luria Bertani broth (1% tryptone, 0.5% yeast extract, 0.5% sodium chloride), cultured at 28°C with 175 rpm shaking for 16 hr, and then resuspended in 10 mM $MgSO_4$ to a final concentration of 1.5×10^8, 1.5×10^6 or 1.5×10^7 cfu/ml as the inoculum for symptom development, in planta bacterial growth, or defence activation assays, respectively. *Arabidopsis* plants were sprayed or leaf-infiltrated with the bacterial suspension, kept moist for 2 days, and then incubated under plant growth conditions. The relative fungal biomass was determined by qPCR as described below. The in planta bacterial population was surveyed by counting the rifampicin-resistant colonies by the dilution-plating method. Three or more samples were assayed for microbial quantification of individual treatments, and all experiments were repeated at least twice.

4.3 | Virus-induced gene silencing in lily

Agrobacterium-mediated infection of TRV-based VIGS vector (Bachan and Dinesh-Kumar, 2012) was used to silence *LsGRP1* in lily. The coding sequence of *LsGRP1* was introduced into the pTRV2 vector to generate pTRV2-LsGRP1. *Agrobacterium tumefaciens* GV3101 was transformed with pTRV1 and pTRV2-LsGRP1 individually, and the bacterial suspensions were prepared to infect plants following the procedure described by Bachan and Dinesh-Kumar (2012). Lily plants with a shoot length of 10–15 cm were treated with the *Agrobacterium* suspension containing 0.05% Silwet L-77 and 200 μM acetosyringone and grown for 4–6 weeks under plant growth conditions before assay. Vector pTRV2 was used instead of pTRV2-Ls-GRP1 in *LsGRP1*-nonsilencing negative control treatment.

4.4 | *Arabidopsis* transformant preparation

The coding sequence of β-glucuronidase (*GUS*) in the binary vector pBI121 (Clontech Laboratories, Inc.) was replaced with the open reading frame of *LsGRP1* to generate a recombinant vector with the expression cassette of 2 × 35S promoter-*LsGRP1*-NOS terminator. *LsGRP1*-transgenic lines were generated from *A. thaliana* accession Col-0 by the flower-dipping method (Clough and Bent, 1998) using *A. tumefaciens* C58C1 transformed with this recombinant vector. The T_5 generations of self-pollinated, homogeneous *LsGRP1* transformants were used in this study.

4.5 | qPCR and RT-qPCR

Plant total DNA and RNA were extracted using a Plant Genomic DNA Purification Kit (GMbiolab Co. Ltd) and a Quick-RNA MiniPrep Kit (Zymo Research Corp.), respectively. The cDNA was synthesized from RNA templates using PrimeScript RT reagent Kit (Takara Bio) at 37 °C for 15 min and 85°C for 5 s. The reverse transcription mixture contained 50 ng/μl RNA, 1 × PrimeScript Buffer, 1 × PrimeScript RT Enzyme Mix I, 25 pM oligo(dT) primer, and 50 pM random hexamers. Quantitative PCR was performed by using the StepOne Real-Time PCR System (Applied Biosystems) and a SensiFAST SYBR Hi-ROX Kit (Bioline Reagents). Quantitative PCR cycling conditions included an initial denaturation of 95°C for 2 min followed by 40 cycles of 95 °C for 5 s and 60°C for 30 s; the reaction mixture contained 50 ng/μl genomic DNA or 5 ng/μl cDNA, 1 × SensiFAST SYBR Hi-ROX Mix, and 400 nM primer pairs. Primer sets for the corresponding amplified targets are listed in Table S1. Three or more samples were used for each quantification. The relative level of amplified targets was calculated using the $2^{-\Delta\Delta Ct}$ method.

4.6 | Western blot analysis

Plant total proteins were extracted with protein extraction buffer (0.2 M 3-(*N*-morpholino)-propanesulfonic acid, pH 7.0, 5% polyvinyl polypyrrolidone, 1% Triton X-100, 10% glycerol, 2% 2-mercaptoethanol, 1 mM phenylmethanesulfonyl fluoride, 1 × proteinase inhibitor cocktail [Sigma-Aldrich Co.]) and subjected to tricine-sodium dodecyl sulphate-polyacrylamide gel electrophoresis (tricine-SDS-PAGE) and western blot analysis as described by Lin and Chen (2014). The relative amounts of target protein bandings recognized by LsGRP1[N] antibody were estimated using the GeneGnome5 Chemiluminescent Western Imaging System (Syngene).

4.7 | Defence inhibitor treatments

Lily leaves were infiltrated with 1 mM 2-DDG, a callose synthesis inhibitor, or 100 μM DPI (prepared in 1% DMSO), a ROS generation inhibitor, at 24–28 hr or 30–60 min before *B. elliptica* inoculation, respectively. Sterile deionized water and 1% DMSO were used instead of 2-DDG and DPI, respectively, as negative treatments.

4.8 | Histochemical staining and quantification of plant defence responses

Leaf samples were subjected to histochemical staining after pathogen inoculation or other treatments. Callose deposition was detected by staining with 0.05% aniline blue in 150 mM KH_2PO_4 solution (pH 9.5). ROS accumulation was detected by staining with 1 mg/ml DAB. In planta fungal growth and plant cell death were

detected by staining with 0.05% trypan blue in lactophenol. Trypan blue staining was performed solely or incorporated with callose or ROS detection before aniline blue staining or after DAB staining, respectively. Chlorophylls were removed from the stained leaves with 75%–95% ethanol. The aniline blue-labelled callose was observed under UV light using a Leica DMIL florescent microscope equipped with a Leica A filter set (band-pass filter 340–380 nm, dichroic mirror 400 nm, long-pass filter 425 nm; Leica Camera AG). The amounts of callose, ROS, and trypan blue-labelled plant cell death were quantified using Photoshop CS6 (Adobe) and ImageJ (National Institutes of Health). Three or more samples were assayed for individual treatments of each detection, and all assays were repeated at least twice.

4.9 | Fungal PCD assay

Chromosomal DNA fragmentation, a typical phenomenon of apoptosis PCD, was detected using TUNEL assay with an in situ Cell Death Detection Kit, Fluorescein (Roche). In vitro assay of fungal apoptosis PCD was performed following the procedure described by Lin *et al.* (2017). The in planta fungal apoptosis PCD was detected following the procedure described below. Plant leaves were collected at different time points after fungal inoculation, fixed with 3.7% formaldehyde in phosphate-buffered saline (PBS, 137 mM NaCl, 2.7 mM KCl, 10 mM Na_2HPO_4, 2 mM KH_2PO_4, pH 7.4) for 24 hr, washed with PBS for 10 min, three times, digested with 50 mg/ml lysing enzymes from *Trichoderma harzianum* (Sigma-Aldrich) in PBS for 1 hr, washed with PBS for 10 min, three times, soaked in permeabilization solution (0.1% Triton X-100, 0.1% sodium citrate) on ice for 30 min, washed with PBS for 10 min, three times, soaked with 50 μl TUNEL solution in the dark at 37°C for 1 hr, treated with 1 μg/ml 4′,6′-diamidino-2-phenylindole (DAPI) in the dark for 10 min, and washed with PBS for 10 min, three times. Then, the leaves were observed under a Leica TCS SP5 II confocal system. Excitation/emission wavelengths for fluorescein-5-isothiocyanate (FITC) and DAPI were 450–490/500–550 mm and 340–390/420–470 nm, respectively. The ratio of FITC-labelled fungal nuclei to DAPI-labelled fungal nuclei was measured to calculate the incidence rate of fungal apoptosis PCD. One hundred DAPI-labelled fungal nuclei were counted in each leaf sample. Three samples were assayed for individual treatments, and the experiments were repeated at least twice.

4.10 | Preparation and application of recombinant proteins

Recombinant proteins of SUMO-LsGRP1, SUMO-LsGRP1ΔC, and SUMO- LsGRP1^C were prepared from *Escherichia coli* C41(DE3) (Lucigen) using the Champion pET SUMO Protein Expression System (Invitrogen) following the procedure described by Lin *et al.* (2017). Among them, SUMO-LsGRP1 and SUMO- LsGRP1ΔC are full-length LsGRP1 and LsGRP1^C-deleted LsGRP1, respectively, fused with an N-terminal portion consisting of a 6 × histidine tag and a yeast SUMO protein SMT3. SUMO-CK fusion partner control protein was prepared from *E. coli* BL21(DE3) (Invitrogen) following the procedure described by Lin *et al.* (2017). Lily leaf disks with a diameter of 18 mm were vacuum-infiltrated with a 10 μM protein solution of SUMO-LsGRP1, SUMO-LsGRP1ΔC, SUMO-LsGRP1^C, or SUMO-CK and air dried for 1 hr before fungal inoculation. Sterile deionized water was used instead of protein solutions as a negative control.

4.11 | Detection of lily response against *B. elliptica* secretion

B. elliptica spores were inoculated into Gamborg broth (0.321% Gamborg's B5 basal salt [Phytotechnology Laboratories LLC], 0.1% glucose) to a final concentration of 200 spores/ml and cultured at 20°C with 175 rpm shaking in the dark for 1 week. Culture supernatant was recovered by filtering through two layers of filter paper (no.1 qualitative filter paper, Advantec Toyo Kaisha Ltd) and 0.45 μm PVDF filter (Millex-HV, Millipore). The filtrate was dialysed in SnakeSkin Dialysis Tubing, 7K MWCO (Thermo Scientific, Inc.) with sterile deionized water to obtain *B. elliptica* secretion. Leaf discs with a diameter of 16 mm prepared from *LsGRP1*-silenced or VIGS-check lily plants were vacuum-infiltrated with *B. elliptica* secretion, washed with sterile deionized water, two times, incubated in 10 ml sterile deionized water in the dark at 20°C, and then subjected to conductivity measurement using a Thermo Scientific Orion 013016MD 2-Electrode Conductivity Cell Probe and aniline blue staining to detect plant cell death and callose deposition, respectively. Five samples were used in individual treatments of each detection and the assay was repeated twice.

4.12 | Evaluation of PTI or ETI activation levels

PTI and ETI activation levels in plants were assessed by measuring PAMP perception-induced callose deposition and ROS accumulation, and effector recognition-induced HR, respectively. For PTI activation assay, the leaves of 8-week-old lily or 25-day-old *Arabidopsis* were infiltrated with 1 μM flg22 (a peptide with a purity >95% synthesized by GenScript USA Inc.) or 10 μM chitohexaose (hexa-*N*-acetylchitohexaose from IsoSep AB). Callose deposition and ROS accumulation in these leaves were microscopically observed at 24 hr after histochemical staining and quantified following the above description. The expression of *Arabidopsis AtrbohD*, which codes for an important PTI-related ROS generator RBOHD (Bigeard *et al.*, 2015; Peng *et al.*, 2018), was detected by RT-qPCR using the primer pairs listed in Table S1. For ETI activation assay, the binary vectors capable of expressing *AvrRpm1* (GeneID: 877422), *AvrRpt2* (GenBank: L11355.1), or *AvrPto* (Gene ID: 1185679) of *P. syringae* were prepared by replacing the *GUS* coding region of vector pBI121 with the open reading frame of these effectors and then separately transforming them into *A. tumefaciens* GV3101. The rosette leaves of 28-day-old *Arabidopsis*

were agroinfiltrated with these *Agrobacterium* transformants individually. Effector recognition-induced HR in agroinfiltrated leaves was visualized by Evans blue staining and quantified using the Evans blue staining-based method described by Jia *et al.* (2016). A *GUS*-deleted pBI121 recombinant vector was used as a blank control. Four samples were assayed for individual treatments of each detection, and all detections were repeated twice at least.

4.13 | Statistical analysis

Statistical analysis was performed using SAS v. 9.2 software (SAS Institute Inc.). Levene's test was used to check the homogeneity of variance. Analysis of variance followed by Fisher's least significant difference test at a significant level of 5% was performed.

DATA AVAILABILITY STATEMENT
The data that support the findings of this study are available from the corresponding author upon reasonable request.

ORCID
Chia-Hua Lin 🆔 https://orcid.org/0000-0002-8614-1095
Chao-Ying Chen 🆔 https://orcid.org/0000-0003-0455-832X

REFERENCES
van Baarlen, P., Staats, M. and van Kan, J.A.L. (2004) Induction of programmed cell death in lily by the fungal pathogen *Botrytis elliptica*. *Molecular Plant Pathology*, 5, 559–574.

van Baarlen, P., Woltering, E.J., Staats, M. and van Kan, J.A.L. (2007) Histochemical and genetic analysis of host and non-host interactions of *Arabidopsis* with three *Botrytis* species: an important role for cell death control. *Molecular Plant Pathology*, 8, 41–54.

Bacete, L., Mélida, H., Miedes, E. and Molina, A. (2018) Plant cell wall-mediated immunity: cell wall changes trigger disease resistance responses. *The Plant Journal*, 93, 614–636.

Bachan, S. and Dinesh-Kumar, S.P. (2012) *Tobacco rattle virus* (TRV)-based virus-induced gene silencing. *Methods in Molecular Biology*, 894, 83–92.

Balint-Kurti, P. (2019) The plant hypersensitive response: concepts, control and consequences. *Molecular Plant Pathology*, 20, 1163–1178.

Balmer, D., Planchamp, C. and Mauch-Mani, B. (2013) On the move: induced resistance in monocots. *Journal of Experimental Botany*, 64, 1249–1261.

Balode, A. and Beļicka, I. (2004) Estimation of *Lilium* resistance against grey mold (*Botrytis* Micheli ex.Fr.). *Agronomijas Vestis*, 7, 134–139.

Bigeard, J., Colcombet, J. and Hirt, H. (2015) Signaling mechanisms in pattern-triggered immunity (PTI). *Molecular Plant*, 8, 521–539.

Chen, C.Y., Lu, Y.Y. and Chung, J.C. (2003) Induced host resistance against Botrytis leaf blight. In: Huang, H.C. and Acharya, S.N. (Eds.) *Advances in Plant Disease Management*. Trivandrum, Kerala, India: Research Signpost, pp. 259–267.

Clough, S.J. and Bent, A.F. (1998) Floral dip: a simplified method for *Agrobacterium*-mediated transformation of *Arabidopsis thaliana*. *The Plant Journal*, 16, 735–743.

Cooper, K.F. (2018) Till death do us part: the marriage of autophagy and apoptosis. *Oxidative Medicine and Cellular Longevity*, 2018, 1–13.

Daughtrey, M.L. and Bridgen, M.P. (2013) Evaluating resistance to *Botrytis elliptica* in field-grown lilies. *Acta Horticulturae*, 1002, 313–318.

Ellinger, D. and Voigt, C.A. (2014) Callose biosynthesis in *Arabidopsis* with a focus on pathogen response: what we have learned within the last decade? *Annals of Botany*, 114, 1349–1358.

Gao, X., Cui, Q., Cao, Q.Z., Zhao, Y.Q., Liu, Q., He, H.B. *et al.* (2018) Evaluation of resistance to *Botrytis elliptica* in *Lilium* hybrid cultivars. *Plant Physiology and Biochemistry*, 123, 392–399.

Giarola, V., Krey, S., von den Driesch, B. and Bartels, D. (2016) The *Craterostigma plantagineum* glycine-rich protein CpGRP1 interacts with a cell wall-associated protein kinase 1 (CpWAK1) and accumulates in leaf cell walls during dehydration. *New Phytologist*, 210, 535–550.

Gottig, N., Vranych, C.V., Sgro, G.G., Piazza, A. and Ottado, J. (2018) HrpE, the major component of the *Xanthomonas* type three protein secretion pilus, elicits plant immunity responses. *Scientific Reports*, 8, 9842.

Gramegna, G., Modesti, V., Savatin, D.V., Sicilia, F., Cervone, F. and De Lorenzo, G. (2016) GRP-3 and KAPP, encoding interactors of WAK1, negatively affect defense responses induced by oligogalacturonides and local response to wounding. *Journal of Experimental Botany*, 67, 1715–1729.

Heil, M. and Baldwin, I.T. (2002) Fitness costs of induced resistance: emerging experimental support for a slippery concept. *Trends in Plant Science*, 7, 61–67.

Hou, P.F. and Chen, C.Y. (2003) Early stages of infection of lily leaves by *Botrytis elliptica* and *B. cinerea*. *Plant Pathology Bulletin*, 12, 103–108.

Hsieh, T.F., Huang, J.W. and Hsiang, T. (2001) Light and scanning electron microscopy studies on the infection of oriental lily leaves by *Botrytis elliptica*. *European Journal of Plant Pathology*, 107, 571–581.

Hückelhoven, R. (2014) The effective papilla hypothesis. *New Phytologist*, 204, 438–440.

Jia, X., Meng, Q., Zeng, H., Wang, W. and Yin, H. (2016) Chitosan oligosaccharide induces resistance to *Tobacco mosaic virus* in Arabidopsis via the salicylic acid-mediated signaling pathway. *Scientific Reports*, 6, 26144.

Jung, N.U., Giarola, V., Chen, P., Knox, J.P. and Bartels, D. (2019) *Craterostigma plantagineum* cell wall composition is remodeled during desiccation and the glycine-rich protein CpGRP1 interacts with pectins through clustered arginines. *The Plant Journal*, 100, 661–676.

Jo, Y. and Cho, W.K. (2018) RNA viromes of the oriental hybrid lily cultivar "Sorbonne". *BMC Genomics*, 19, 748.

Kanyuka, K. and Rudd, J.J. (2019) Cell surface immune receptors: the guardians of the plant's extracellular spaces. *Current Opinion in Plant Biology*, 50, 1–8.

Lin, C.H. and Chen, C.Y. (2014) Characterization of the dual subcellular localization of *Lilium* LsGRP1, a plant class II glycine-rich protein. *Phytopathology*, 104, 1012–1020.

Lin, C.H. and Chen, C.Y. (2017) The pathogen-inducible promoter of defense-related *LsGRP1* gene from *Lilium* functioning in phylogenetically distinct species of plants. *Plant Science*, 254, 22–31.

Lin, C.H., Chang, M.W. and Chen, C.Y. (2014) A potent antimicrobial peptide derived from the protein LsGRP1 of *Lilium*. *Phytopathology*, 104, 340–346.

Lin, C.H., Pan, Y.C., Liu, F.W. and Chen, C.Y. (2017) Prokaryotic expression and action mechanism of antimicrobial LsGRP1[C] recombinant protein containing a fusion partner of small ubiquitin-like modifier. *Applied Microbiology and Biotechnology*, 101, 8129–8138.

Liu, Y.H., Huang, C.J. and Chen, C.Y. (2008) Evidence of induced systemic resistance against *Botrytis elliptica* in lily. *Phytopathology*, 98, 830–836.

Liu, Y.H., Huang, C.J. and Chen, C.Y. (2010) Identification and transcriptional analysis of genes involved in *Bacillus cereus*-induced systemic resistance in *Lilium*. *Biologia Plantarum*, 54, 697–702.

Lorang, J.M. (2019) Necrotrophic exploitation and subversion of plant defense: a lifestyle or just a phase, and implications in breeding resistance. *Phytopathology*, 109, 332–346.

Lu, Y.Y. and Chen, C.Y. (1998) Probenazole-induced resistance of lily leaves against *Botrytis elliptica*. *Plant Pathology Bulletin*, 7, 134–140.

Lu, Y.Y. and Chen, C.Y. (2005) Molecular analysis of lily leaves in response to salicylic acid effective towards protection against *Botrytis elliptica*. *Plant Science*, 169, 1–9.

Lu, Y.Y., Liu, Y.H. and Chen, C.Y. (2007) Stomatal closure, callose deposition, and increase of *LsGRP1*-corresponding transcript in probenazole-induced resistance against *Botrytis elliptica* in lily. *Plant Science*, 172, 913–919.

Mangeon, A., Pardal, R., Menezes-Salgueiro, A.D., Duarte, G.L., de Seixas, R., Cruz, F.P. *et al.* (2016) *AtGRP3* is implicated in root size and aluminum response pathways in *Arabidopsis*. *PLoS ONE*, 11, e0150583.

Mangeon, A., Menezes-Salgueiro, A.D. and Sachetto-Martins, G. (2017) Start me up: revision of evidences that AtGRP3 acts as a potential switch for AtWAK1. *Plant Signaling & Behavior*, 12, e1191733.

Mauch-Mani, B., Baccelli, I., Luna, E. and Flors, V. (2017) Defense priming: an adaptive part of induced resistance. *Annual Review of Plant Biology*, 68, 485–512.

McRae, E.A. (1998) Oriental lily hybrids. In: McRae, E.A. *Lilies: a guide for growers and collectors*. Portland: Timber Press, pp. 239–257.

Noman, A., Aqeel, M. and Lou, Y. (2019) PRRs and NB-LRRs: from signal perception to activation of plant innate immunity. *International Journal of Molecular Sciences*, 20, 1882.

de Oliveira, D.E., Seurinck, J., Inzé, D., Van Montagu, M. and Botterman, J. (1990) Differential expression of five *Arabidopsis* genes encoding glycine-rich proteins. *The Plant Cell*, 2, 427–436.

Park, A.R., Cho, S.K., Yun, U.J., Jin, M.Y., Lee, S.H., Sachetto-Martins, G. *et al.* (2001) Interaction of the *Arabidopsis* receptor protein kinase Wak1 with a glycine-rich protein, AtGRP-3. *Journal of Biological Chemistry*, 276, 26688–26693.

Peng, Y., van Wersch, R. and Zhang, Y. (2018) Convergent and divergent signaling in PAMP-triggered immunity and effector-triggered immunity. *Molecular Plant-Microbe Interactions*, 31, 403–409.

Shlezinger, N., Doron, A. and Sharon, A. (2011a) Apoptosis-like programmed cell death in the grey mold fungus *Botrytis cinerea*: genes and their role in pathogenicity. *Biochemical Society Transactions*, 39, 1493–1498.

Shlezinger, N., Minz, A., Gur, Y., Hatam, I., Dagdas, Y.F., Talbot, N.J. *et al.* (2011b) Anti-apoptotic machinery protects the necrotrophic fungus *Botrytis cinerea* from host-induced apoptotic-like cell death during plant infection. *PLoS Pathogens*, 7, e1002185.

Staats, M., van Baarlen, P. and van Kan, J.A. (2005) Molecular phylogeny of the plant pathogenic genus *Botrytis* and the evolution of host specificity. *Molecular Biology and Evolution*, 22, 333–346.

van Tuyl, J.M. and Arens, P. (2011) *Lilium*: breeding history of the modern cultivar assortment. *Acta Horticulturae*, 900, 223–230.

Ueki, S. and Citovsky, V. (2002) The systemic movement of a tobamovirus is inhibited by a cadmium-ion-induced glycine-rich protein. *Nature Cell Biology*, 4, 478–486.

Ueki, S. and Citovsky, V. (2005) Identification of an interactor of cadmium ion-induced glycine-rich protein involved in regulation of callose levels in plant vasculature. *Proceedings of the National Academy of Sciences of the United States of America*, 102, 12089–12094.

Veloso, J. and van Kan, J.A.L. (2018) Many shades of grey in *Botrytis*–host plant interactions. *Trends in Plant Science*, 23, 613–622.

de Vleesschauwer, D., Gheysen, G. and Höfte, M. (2013) Hormone defense networking in rice: tales from a different world. *Trends in Plant Science*, 18, 555–565.

de Vleesschauwer, D., Xu, J. and Höfte, M. (2014) Making sense of hormone-mediated defense networking: from rice to *Arabidopsis*. *Frontiers in Plant Science*, 5, 611.

Voigt, C.A. (2014) Callose-mediated resistance to pathogenic intruders in plant defense-related papillae. *Frontiers in Plant Science*, 5, 168.

Walters, D. and Heil, M. (2007) Costs and trade-offs associated with induced resistance. *Physiological and Molecular Plant Pathology*, 71, 3–17.

Wang, X., Jiang, N., Liu, J., Liu, W. and Wang, G.L. (2014) The role of effectors and host immunity in plant-necrotrophic fungal interactions. *Virulence*, 5, 722–732.

Xu, H., Xu, L., Yang, P., Cao, Y., Tang, Y., He, G. *et al.* (2019) Virus-induced *Phytoene Desaturase* (*PDS*) gene silencing using *Tobacco rattle virus* in *Lilium* × *formolongi*. *Horticultural Plant Journal*, 5, 31–38.

Yang, E.J., Oh, Y.A., Lee, E.S., Park, A.R., Cho, S.K., Yoo, Y.J. *et al.* (2003) Oxygen-evolving enhancer protein 2 is phosphorylated by glycine-rich protein 3/wall-associated kinase 1 in *Arabidopsis*. *Biochemical and Biophysical Research Communications*, 305, 862–868.

Zhang, W., Zhao, F., Jiang, L., Chen, C., Wu, L. and Liu, Z. (2018) Different pathogen defense strategies in *Arabidopsis*: more than pathogen recognition. *Cells*, 7, 252.

SUPPORTING INFORMATION

Additional supporting information may be found online in the Supporting Information section.

How to cite this article: Lin C-H, Pan Y-C, Ye N-H, Shih Y-T, Liu F-W, Chen C-Y. LsGRP1, a class II glycine-rich protein of *Lilium*, confers plant resistance via mediating innate immune activation and inducing fungal programmed cell death. *Molecular Plant Pathology*. 2020;21:1149–1166. https://doi.org/10.1111/mpp.12968